# A DIVERGING COLLIMATOR FOR GAMMA-RAY IMAGING CAMERAS

G. Muehllehner

*Nuclear-Chicago Corporation, Des Plaines, Illinois*

With the advent of stationary scintillation cameras a new powerful tool became available which offers significant improvement over scanning gamma-ray detectors. Cameras image radioisotope distributions in a much shorter time than scanners and also make dynamic studies possible. One disadvantage, however, is that their field of view is presently limited to a diameter of approximately 10 in. while the scanner can view an area appreciably bigger than that. Thus it is often necessary to take two exposures when imaging large objects such as the lungs. This lengthens the total exposure time and introduces additional problems such as how to determine accurately the relative position of the two exposures.

These problems can be solved by constructing a larger scintillation detector for the camera. However, the technical problems involved increase quickly with increasing diameter. A second solution, described and evaluated in this paper, consists of making a special collimator that can be added to a camera with a useful detector diameter of 10 in. to increase its field of view so that large objects can be imaged.

## PERFORMANCE CHARACTERISTICS

The diverging collimator is a multihole collimator with radially diverging holes of uniform diameter. The converging side faces the camera while the diverging side faces the object to be imaged. A cross-sectional view through the collimator is shown schematically in Fig. 1. Image planes at varying distances from the collimator are indicated, showing the increase in the diameter of the imaged area.

**Efficiency.** As in the case of parallel-hole collimators (*1*), the geometric efficiency is calculated by considering a plane source in contact with the collimator and is given to a good approximation by

$$g_0 = \frac{d^2}{a'^2_e} \frac{K^2 d^2}{(d+t)^2} \qquad (1)$$

where K depends on the shape of the holes and their distribution pattern, d is the diameter of the hole, t is the septal thickness as indicated in Fig. 1 and $a'_e$ is the effective length of the hole which is dis-

Received June 6, 1968; revision accepted Sept. 24, 1968.

For reprints contact: G. Muehllehner, Research Dept., Nuclear-Chicago Corp., 333 E. Howard Ave., Des Plaines, Ill.

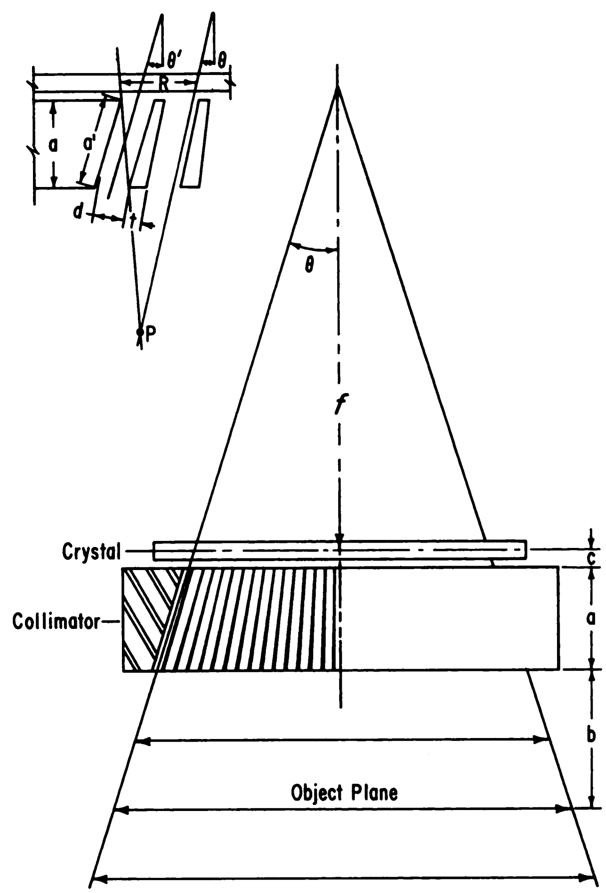


**FIG. 1.** Cross-section through diverging collimator showing several object planes. Insert shows partial section through diverging collimator which gives dimensions used in text (insert not to scale).

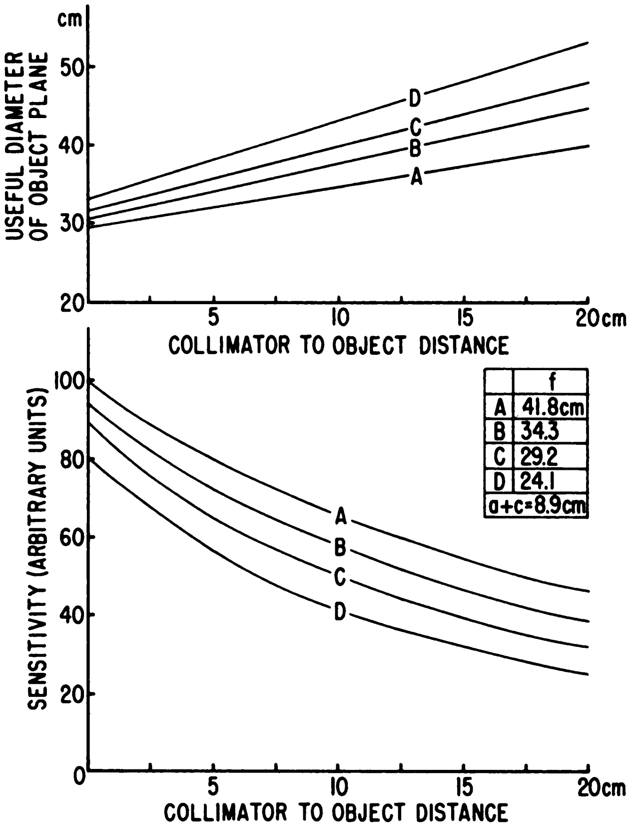


**FIG. 2.** Field of view and sensitivity as a function of collimator-to-object distance for collimators with several focal lengths. Diameter of field of view was calculated using useful scintillation detector diameter of 24.1 cm.

cussed below. The first factor in Eq. 1 is proportional to the solid angle subtended by the scintillation crystal for a point source located in the source plane under a hole (it is assumed that $a'_e \gg d$); the second factor is proportional to the fraction of the plane source not covered by the septa.

If the source is always larger than the area viewed, the efficiency is independent of depth as has been shown for both parallel-hole and focused collimators (*2,3*). The same argument applies here: while the solid angle decreases as the square of the distance from the scintillator, the area "viewed" by each hole increases as the square of this distance. Therefore the product of the two factors is independent of this distance.

For a source that is smaller than the total imaged area, however, the efficiency decreases proportionally as the imaged area increases. The imaged area varies as a function of the collimator-to-object-plane distance b according to

$$A = A' \left[ \frac{f + a + b + c}{f + a + c} \right]^2 \qquad (2)$$

where A′ is the useful area at the outside surface of the collimator; f, a, b and c are shown in Fig. 1. The geometric efficiency is then given by

$$g = g_0 \frac{A'}{A} = \left[ \frac{Kd^2}{a'_e(d + t)} \right]^2 \left[ \frac{f + a + c}{f + a + b + c} \right]^2. \qquad (3)$$

Figure 2 shows a plot of g as a function of b for a number of focal lengths.

**Uniformity of efficiency.** If the hole diameter is kept constant over the full diameter, then the only quantity in Eq. 3 which is dependent on the radial distance from the center is $a'_e$ which is given by

$$a'_e = a_e / \cos \theta \qquad (4)$$

where $a_e$ is the effective collimator thickness which is smaller than a by twice the mean free path of the gamma rays in the collimator material (*4*). The geometric efficiency thus falls off as $\cos^2 \theta$. For the examples shown in Fig. 2 the maximum variation over the useful diameter which this introduces is ±4%, ±6%, ±8% and ±12% for A, B, C and D, respectively.

The sensitivity of the camera, however, varies linearly as the detection efficiency of the crystal. Since the path length of the gamma rays increases with increasing radius, the detection efficiency also increases. For low-energy gamma rays this increase has a negligible effect; however, at higher energies (above 300 keV) this effect results in an increase in sensitivity at larger radii which is approximately proportional to $\cos \theta$. Thus the numbers given above for the variation in geometrical efficiency are reduced by up to half their values when over-all sensitivity is considered.

**Resolution.** The geometric resolution for a point source P (Fig. 1) as previously defined (*5*) can be shown to be

$$R = \frac{(a_e + b + c)d}{a_e} \frac{1}{\cos \theta} - (a_e + b + c)(\tan \theta' - \tan \theta) \qquad (5)$$

where the symbols used are given in Fig. 1. The first term is identical to the resolution given for parallel-hole collimators except for the $1/\cos \theta$ term. The second term is a correction term due to the fact that the angle of inclination of the holes changes with radial distance. In terms of the focal length the resolution is given by

$$R_0 = MR = \frac{f + a_e + b + c}{f} R = \frac{(a_e + b + c)d}{a_e} \frac{1}{\cos \theta} \left[ 1 + \frac{a_e + 2c}{2f} \right] \qquad (6)$$

where $R_0$ is the resolution distance in the object plane which is equal to the resolution at the crystal R multiplied by the minification factor M,

$$M = \frac{f + a_e + b + c}{f}. \qquad (7)$$

Again Eq. 6 consists of a term identical to the resolution for the parallel-hole collimator including the $1/\cos\theta$ term and a correction term which goes to zero as f goes to infinity. For the examples given in Fig. 2 the correction term is 12%, 15%, 17% and 21% for A, B, C and D, respectively. A slight radial asymmetry in the resolution distance has not been included in this formulation.

## EXPERIMENTAL EVALUATION

Two factors were considered of overriding importance in the selection of parameters for the construction of our diverging collimator. First, its useful field should be large enough to allow the lungs of most patients to be imaged with a single exposure; and second, loss of resolution and nonuniformity of efficiency should be kept to a minimum.

Since approximately 95% of all lungs can be imaged if the field of view has a diameter of 15 in. (*6*) and since this diameter is required at a depth of approximately 10 cm, a focal length of 34.3 cm was chosen (Example B of Fig. 2). For an object distance of 10 cm, the imaged area is increased by a factor of more than two compared to the area imaged by the parallel-hole collimator. Geometric resolution is degraded by 15% compared to the equivalent parallel-hole collimator (correction term in Eq. 6) and the nonuniformity of efficiency is less than ±6% as stated above. Collimator thickness (3 in.), hole diameter (0.247 in.) and hole arrangement were kept close to those of the existing medium-energy, parallel-hole collimator to allow an experimental comparison between the two collimators. The diverging collimator is intended for a maximum gamma-ray energy of 0.41 MeV. All measurements were made using a Pho/Gamma scintillation camera (Nuclear-Chicago Corp.).

**Efficiency.** The geometric efficiency of the diverging collimator was measured indirectly by measuring over-all sensitivity (counts per unit time per unit of source activity) of the camera system with both parallel-hole and diverging collimators and comparing the two sets of data. Sensitivity with the diverging collimator was measured both as a function of radial distance from the center and as a function of object-to-collimator distance using an extended source. The source consisted of a circular piece of filter paper 1 in. in diameter which was soaked in a solution of $^{133}Ba$ which has a primary gamma-ray energy of 355 keV. The results of these measurements are shown in Fig. 3 together with a radial sensitivity profile measured with the parallel-hole collimator for an object distance of 10 cm. An extended source was used because small variations in sensitivity due to the hole pattern and the finite size of the holes are averaged out. The use of the extended source, however, has the disadvantage that as the source is moved across the edge of the useful field, the measured sensitivity begins to drop off gradually over a radial distance of 1 in. even if the fall-off in sensitivity is abrupt. If the source is placed at the edge of the useful field, half of the source is inside the field of view and the other half outside, resulting in a drop in sensitivity of 50%. For this reason the figures quoted as useful diameter in Fig.

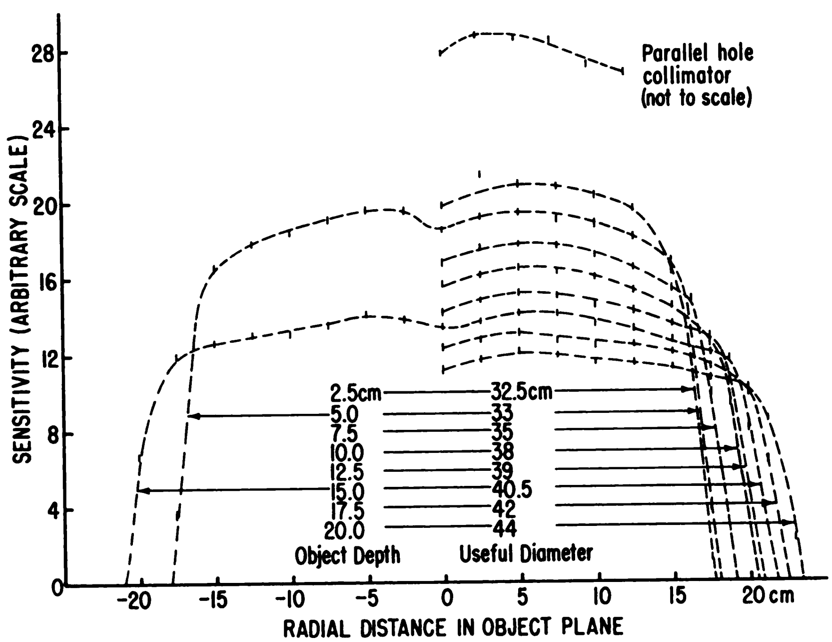


**FIG. 3.** Sensitivity measured as a function of radial distance and collimator-to-object distance. Dashed lines are smooth lines through data points only.

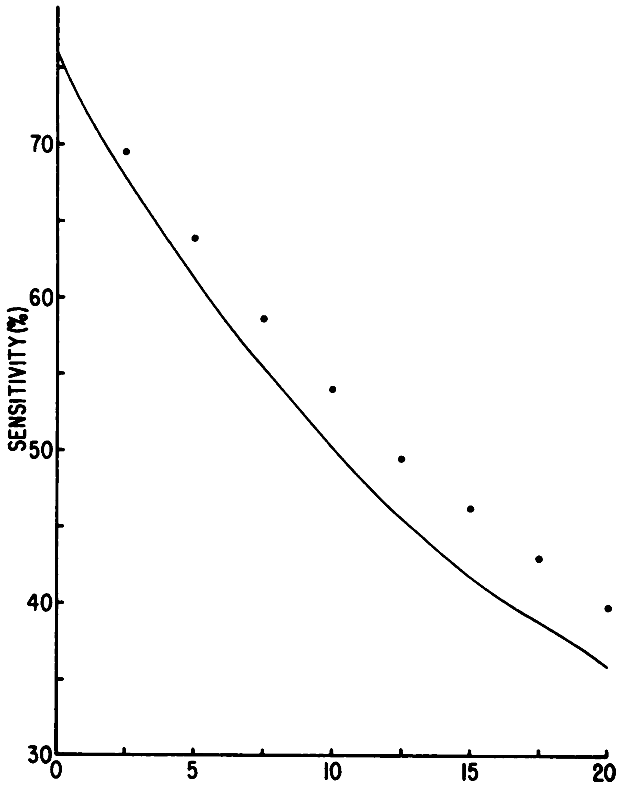


**FIG. 4.** Sensitivity as function of collimator-to-object distance normalized to sensitivity of parallel-hole collimator. Solid line represents calculated curve.

3 are measured at the 50% points. The measured useful diameters agree well with the values given for Example B in Fig. 2.

If the reasonable assumption is made that radial variations in sensitivity with the parallel-hole collimators are due to nonuniformities in the sensitivity of the detector (there is no reason to believe that the parallel-hole collimator introduces any variation in sensitivity) and if the diverging-collimator data are therefore normalized to the parallel-hole collimator data, then the variation in sensitivity is within ±4% over the useful diameter. This variation is attributed to variation in geometric efficiency of the collimator and is in good agreement with the predicted value of less than ±6%.

The variation of sensitivity with collimator-to-object-plane distance is plotted in Fig. 4. To show the loss in sensitivity compared to the sensitivity obtained with the parallel-hole collimator, the data were normalized to the sensitivity measured with the parallel-hole collimator. The calculated values take into account small differences in hole diameter and septal thickness between the two collimators.

**Resolution.** For the resolution measurements a 10-in.-long line source of $^{133}Ba$ was placed along an axis of the camera (even though the crystal is axially symmetrical, a set of axes is defined by the position of the photomultiplier tubes and the position matrix) and the position signals were analyzed with a two-parameter multichannel analyzer in such a way that the resolution could be determined for several positions along the axis simultaneously. The results were multiplied by the inverse of the minification factor to obtain the resolution (FWHM) in the object plane. They are plotted in Fig. 5 for several collimator-to-object distances together with the calculated values. The calculated values were obtained using Eq. 6; a constant intrinsic resolution of 8 mm was assumed.

Equation 6 was obtained by assuming the source to be a point source. The point-source response function p(x,y) is conical in shape and different from the line-source response function L(x). Therefore L(x) was calculated from p(x,y) by performing the integration (7)

$$L(x) = \int_{-\infty}^{+\infty} p(x,y)\,dy. \qquad (8)$$

The full-width-at-half-maximum (FWHM) values for the point and line-source response functions were found to be approximately equal.

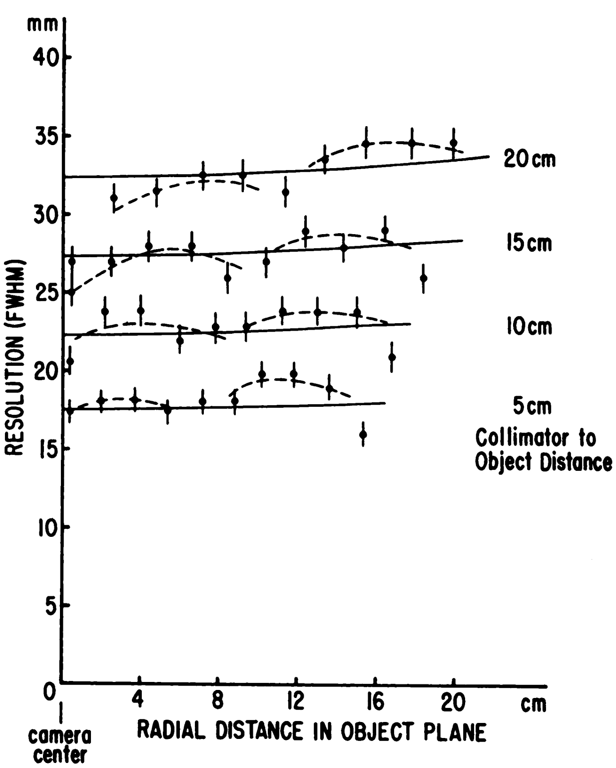


**FIG. 5.** Resolution as function of radial distance and collimator-to-object distance measured with $^{133}Ba$ line source. Solid lines represent calculated values and dashed lines represent variation apparently introduced by detector.

The experimentally determined points do, of course, include variations in resolution of the camera. To determine their size, the collimator and the line source were rotated 90 deg, and the experiment was repeated. It was concluded that the variation in resolution indicated by the dashed lines in Fig. 5 is a result of the arrangement of the photomultiplier tubes along the axis of the measurement since the pattern was different along the other axis. As the object-to-collimator distance is increased, the minification and therefore the contribution of the inherent resolution to the total resolution is also increased. For this reason the pattern appears just as prominently at 20 cm as it does at 5 cm.

If the experimental resolution values are averaged radially and compared to an average calculated resolution, then the theoretical and experimental values for resolution as a function of object-to-collimator distance agree to within 2%.

The same resolution measurement was repeated for the parallel-hole collimator, and the agreement between the experimental and calculated values is equally good. If intrinsic resolution is taken into account, calculations predict a difference of 20% between the total resolution using the diverging collimator and the parallel-hole collimator for all object-to-collimator distances between 2.5 and 20 cm; this has indeed been confirmed experimentally.

## SUMMARY

The diverging collimator gives a field of view that is large enough for practically all clinical applications. It can be used with existing 10-in.-diameter cameras, thus largely eliminating the need for larger-diameter detectors which would either be more costly or show poorer resolution and uniformity. The larger field of view is traded off for only a 20% loss in resolution and a reduction in efficiency which is proportional to the increase in the field of view. Uniformity of resolution and efficiency over the useful object plane is well within acceptable limits and has approximately the same magnitude as non-uniformities in the camera itself.

**Note added in proof:** After this article was written, a second diverging collimator was constructed which has a smaller field of view (13 in. at an object distance of 4 in.) but a higher resolution (improved by 20%). This collimator will be the subject of a later communication.

## ACKNOWLEDGMENT

After this work was under way, it was brought to the author's attention that the construction of a diverging collimator had been suggested previously (*8*). The author wishes to express his gratitude to W. G. Walker and J. R. Wolff as well as to H. O. Anger for many valuable discussions regarding the design and evaluation.

## REFERENCES

*1.* ANGER, H. O.: Survey of radioisotope cameras. *ISA Transactions* **5**:311, 1966.

*2.* WALKER, W. G.: Private communication.

*3.* HINE, G. J.: Evaluation of focused collimator performance. *Intern. J. Appl. Radiation Isotopes* **18**:815, 1967.

*4.* MATHER, R. L.: Gamma-ray collimator penetration and scattering effects. *J. Appl. Phys.* **28**:1,200, 1957.

*5.* ANGER, H. O.: Scintillation camera with multichannel collimators. *J. Nucl. Med.* **5**:515, 1964.

*6.* GOTTSCHALK, A.: Private communication.

*7.* KELLER, E. L. AND COLTMAN, J. W.: Modulation transfer and scintillation limitations in gamma-ray imaging. *J. Nucl. Med.* **9**:537, 1968.

*8.* ANGER, H. O.: Scintillation camera. *Rec. Sci. Instr.* **29**:27, 1958.